Building and Environment 243 (2023) 110707

Contents lists available at ScienceDirect

Building and Environment

journal homepage: www.elsevier.com/locate/buildenv

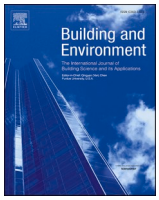

Studying the influence of surface properties on the cell attachment and anti-fouling capacity of Ag/SiO_2 superhydrophobic coatings for building materials

Rafael Zarzuela [b,*], Marcia Domínguez [a], María Carbú [c], Ignacio Moreno-Garrido [d], Ana Diaz [b], Jesús M. Cantoral [d], M.L. Almoraima Gil [b], María J. Mosquera [b]

[a] Instituto Interuniversitario de Investigación de Reconocimiento Molecular y Desarrollo Tecnológico (IDM), Universitat Politècnica de València, Universitat de València, Valencia, Spain
[b] Department of Physical Chemistry, Faculty of Sciences, Universidad de Cádiz, Campus Río San Pedro s/n, 11510, Puerto Real, Cádiz, Spain
[c] Microbiology Laboratory, Faculty of Marine and Environmental Sciences, Universidad de Cádiz, 11510, Puerto Real, Spain
[d] Institute of Marine Sciences of Andalucía, (CSIC), Campus Río San Pedro, s/n, 11510, Puerto Real, Cádiz, Spain

ARTICLE INFO

Keywords:
Anti-microbial
Functional surface
Super hydrophobic
Biocide
Bacterial adhesion
Building materials

ABSTRACT

Anti-fouling coatings are a common solution for the protection of porous building materials from the effects of microbial colonization over their functionality and durability. Usually, this is achieved through the incorporation of biocides or the passive control by reducing bioreceptivity. Superhydrophobic surfaces are considered a promising strategy due to their reported capacity for reducing cell adhesion, but their affinity to non-polar substances may decrease their effectiveness under the right circumstances (e.g. organic contamination, cell walls with hydrophobic domains). The combination of these surfaces with active biocides may compensate these drawbacks, however, a close contact with the microorganisms is necessary to promote their effect.

This work studies the factors that determine the anti-fouling capacity of a coating, tested on porous building materials, that combines superhydrophobic surface with a nanostructured Ag/SiO_2 biocide agent. Special attention is paid to understanding to which extent the cell-surface interactions modulate the initial cell attachment to the surface and the biocidal effect. To this end, the electrostatic forces and surface energy balance were considered using different reference bacteria and a yeast. The results indicate that the hydrophobic character of the surface favors the cell attachment and the biocide agent may be unable to fully compensate this effect for all microorganisms. In addition, changes in micro and nano roughness seem to play an equally significant role. Overall, this study aims to provide a theoretical and experimental insight to assist in the future design of anti-fouling coatings tailored to the organisms responsible of fouling processes.

1. Introduction

Biological contamination of the materials that conform everyday objects and structures is associated to a plethora of problems, ranging from the spread of diseases (e.g. fomites, fungal infections, food contamination) [1–5] to the alteration and decay of building elements [6–9], which have a negative impact on their functionality and service life. These issues entail considerable efforts and costs in the form of cleaning, maintenance and rehabilitation actions. The effects of biofouling on building materials include, but are not limited to: (1) aesthetical alterations of the surface; (2) Negative changes to the material functionality; (3) Structural damages to the material by physical-chemical processes. Such damages are accelerated when the materials are exposed to outdoors environments, where biological, physical and chemical agents tend to act in synergy [8]. Water, aside from being necessary for microbial growth, is associated to a number of decay processes, either as vehicle of other agents (e.g. soluble salts) or by direct action mechanisms such as freeze/thaw cycles, leaching of soluble minerals from the structure or solubilization of carbonates by acid rain [10,11]. These processes lead to structural damages in the form of delaminations, pitting, granular disintegration, cracks or increased porosity, which in turn increase the water absorption capacity and bioreceptivity of the materials. Simultaneously, the damages caused by biofouling may increase the material susceptibility to weathering.

* Corresponding author.
E-mail address: rafael.zarzuela@uca.es (R. Zarzuela).

https://doi.org/10.1016/j.buildenv.2023.110707
Received 23 May 2023; Accepted 4 August 2023
Available online 5 August 2023

Aside from the material damages associated to biofouling, contaminated building materials may contribute to spreading diseases through different mechanisms [1–5]. A prime example of these is the cross-contamination of food sources in contact with kitchen surfaces, one of the most common transmission methods of gastrointestinal pathogens (e.g. *Listeria monocytogenes*, *Salmonella* spp.). The hazards for human health become more evident indoors, especially in damp areas with poor ventilation. Examples of these include respiratory mycoses after prolonged exposure to fungal spores from black mold nad mildew [12], or the systemic symptoms of the "sick building syndrome" [3,4], associated to the inflammatory response to fungal spores, mycotoxins and volatile compounds released by bacteria.

The biodeterioration process of building materials is complex and involves a sequence of microorganisms such as bacteria, cyanobacteria or meristematic fungi as first colonizers and algae, filamentous fungi, lichens, mosses and vascular plants as secondary colonizers [8,13].

Fungi are often found in altered building materials, exposed to high humidity and have been identified as one of the main causes of biodeterioration by chemical and mechanical mechanisms, in addition to their effects on aesthetic alteration due to the production of pigments. Concerning mechanical deterioration, expansion of the fungal hyphae can exert pressure between the mineral grains and structural defects (i.e. cracks, macropores), penetrating into the structure and causing loss of cohesion. This mechanism is especially remarkable for endolithic fungi, which can produce pitting phenomena [12,14]. The chemical action of fungi seems to be the most important degradation, as research shows a close relationship between the solubility of the substrate and the decrease in pH, due to the production organic acids as secondary metabolites (e.g. citric, oxalic, gluconic, glucuronic, lactic, fumaric) that form chelation complexes with the metal cations of the substrate, dissolving carbonates, silicates (mica and orthoclase), minerals containing iron and magnesium (biotite, olivine, pyroxene) and various phosphates. In addition to the material decay, fungi are one of the main caused of color alteration and may negatively affect the indoor environment by releasing volatile, bad-smelling compounds, mycotoxins and spores.

The role of algae and cyanobacteria [15–17] in biodeterioration of building materials has been mostly attributed to aesthetical alterations, and their ability to enable the growth of heterotrophic organisms by providing a source of organic matter and creating a favorable environment through the secretion of extracellular polymeric substances (EPS). However, research has shown that these microorganisms may also induce chemical and physical degradation [15,16]. These mechanisms, though, are generally less aggressive than fungi and difficult to identify in exposed materials.

Bacteria are a group of colonizers with relatively simple nutritional and ecological needs, which easily develop on building elements exposed to the elements, especially when their moisture content is high. The bacteria that settle on the surface of the building can be divided into the so-called chemoautotrophs or chemosynthetic, which comprise the sulfur cycle bacteria (sulfate-reducing and sulfoxide), the nitrogen cycle bacteria and ferrobacteria, and, on the other hand, the heterotrophic bacteria [8,13,18]. Sulfur cycle bacteria are mostly found on materials subject to air pollution and sewer systems, where sulfur dioxide together with hydrogen sulfide produces sulfur compounds on the substrate (e.g. sulfates, gypsum), which favors their growth. Nitrogen cycle bacteria are most common in elements in contact with soil, and are able to degrade the materials through oxidation processes, from which they obtain their energy, and the production of nitric acid as result of their metabolism. Heterotrophic bacteria also play a very important role in the degradation of building materials, specially on its earlier stages as many of them are able to grow using organic contaminant deposits as a carbon source. They can exert their action through the formation of carbon dioxide and organic acids that, although relatively weak, can damage carbonate minerals from the substrate [4,6,18]. The formation of black scabs, brown patina, and exfoliation are examples of direct decay phenomena associated to bacteria, although their main influence in biofouling is generally associated to their role as first colonizers that provide organic matter for heterotrophs and create a favorable environment through the secretion of extracellular substances.

A preventive strategy against the proliferation of microorganisms on building materials is the application of surface treatments or coatings incorporating of biocidal components. To this regard, metallic nanoparticles (Ag, Cu, functionalized Au …) and oxide nanoparticles (CuO, ZnO, SiO_2 …) have emerged in the recent years as broad spectrum biocidal agents [19–22] with lower chance of promoting the apparition of drug-resistant organisms. Another advantage of these biocides is the ability to incorporate them in many types of matrices, including organic coatings, sol-gel systems, cementitious materials or as dispersions in water or solvents [19]. Among the oxide nanoparticles, TiO_2 has been thoroughly studied for the photo-disinfection of surfaces [23], including medical equipment and fabrics. The TiO_2 photocatalytic effect generates reactive oxygen species that produce oxidative stress on the pathogens resulting in their elimination [24]. Silver nanoparticles (AgNPs) are among the most widely used for their excellent antibacterial and antifungal properties [25–27]. Its mechanisms of action include: (1) those related to the release of Ag^+ ions, which denature DNA, proteins and alter cellular respiration, and (2) those specific to NPs that lead to the generation of ROS, direct physical damage, disturbance of membrane/wall permeability. The use of biocides based on metal/metal oxides, however, is not exempt of limitations, as their effect depends on the dosage and distribution on the surface, and leaching processes may lead to a loss of performance over time and release to the environment of components toxic for aquatic organisms [28].

Alternative anti-fouling strategies rely on passive mechanisms to control biofilm formation on its different stages [29–31], either by limiting water/moisture retention with hydrophobic materials, reducing the build-up of organic contaminants, decreasing surface porosity or by modifying the adhesion between the surface and the cells. The first stage of biofilm formation involves the adhesion of the microorganisms (commonly bacteria or microalgae) to the surface through physical forces, which depends on a number of factors [32] related to: (1) The composition of the material and cell walls, which determine the magnitude of attractive or repulsive forces (i.e. electrostatic, Van der Waals, Hydrogen bonds). (2) Surface roughness, which generally increases the effective area, and morphology of the topographical features. (3) Exposure conditions, including mode of contamination (e.g. rainfall, aerosols, flooded elements), flow conditions (e.g. pipe systems) and composition of the media (e.g. salinity, organic matter content).

Among the eco-friendly methods to control biofouling, superhydrophobic surfaces have attracted attention in recent years [33–35]. These surfaces combine a low surface energy and regular micro- or nano-roughness, leading to high contact angles (>150°) and water repellence. Their hydrophobic character decreases the absorption of water and soluble species (e.g. oligo elements, nitrogen sources) in porous materials, prevent microbial growth, while decreasing the affinity for polar EPS. In addition, these surfaces are defined by a Cassie-Baxter state, characterized by the entrapment of air pockets between the roughness valleys and water, which leads to a decrease of the effective area for attachment of cells and pollutants and facilitates the detachment of biofilms. On the flip side, these surfaces can sometimes be ineffective and even promote biological colonization [36]. This may be due to the limited stability of the Cassie-Baxter state, which can be easily perturbed by contaminants (biogenic or abiotic) or physical damages to the topography, leading to a Wenzel wetting regime. Under these circumstances, cell and EPS adhesion may actually increase due to their high roughness and the differences in the microorganism-substrate interfacial tension in comparison with a hydrophilic surface [37,38]. Multiple studies have shown that [32,37,39], in some aqueous systems, the adhesion of different microorganisms to a surface can increase on materials with a low surface energy. This has been explained in basis of surface free energy balance by OWRK model and Good's geometrical

mean equation [32,39], as the cell walls have a high contribution of the dispersive (non-polar) components, and more detailed analysis using extended DLVO theory [32,37] have reached similar conclusions. However, contradictory experimental results are found in literature [32] due to the influence of multiple factors on bacterial attachment (roughness, ionic strength of the media, bacterial motility and rigidity, hydrodynamic conditions …) [32]. Considering how the surface properties of cells (polarity, electrostatic charge, hydrophobicity) vary enormously from one microorganism to another, it is difficult to predict the anti-fouling effectiveness of strategies based on surface modification.

A possible solution to the limitations raised above is the combination of superhydrophobic surfaces with actives biocides in such a way that the superhydrophobic surface would modulate cell adhesion and limit water absorption, while the biocidal agent would enhance anti-fouling performance at longer exposure intervals. The combination of these surfaces with nano-biocides has been reported in different materials including fabric [38,40,41] or metals [42–44], and our previous reports show potential application on building materials [45,46]. At the same time, the effect of nano-biocides is also dependent on their capacity to interact with the cell structures [47,48], and is generally favored as the attraction forces increase. Thus, changes in surface-cell adhesion forces can lead to opposing effects related to the initial (passive) cell attachment and cell survivability. In our previous works [39,46], we found that the incorporation of AgNPs in a superhydrophobic coating was able to offset the increased adhesion of cyanobacteria and microalgae after the surface switched to a Wenzel state, but contradicting results were obtained in tests with *Gram* - bacteria and a yeast on organically modified silica (ormosil) xerogels.

This work aims to evaluate and understand the factors that determine the antifouling efficacy of a superhydrophobic and biocidal multifunctional surface treatment formulated for the protection building materials, focusing on the physical interactions (electrostatic, interfacial tensions) of the biocide component and the coated surfaces with the microorganisms and considering topography aspects, wetting properties and toxicity of the biocide. While the individual effect of these factors is well-known, their combination is seldom considered in the design of anti-fouling coatings. To this end, the study was performed on mortars treated with ormosil-based coatings containing Si/AgNPs modified to obtain a positive charge to increase their contact with the cell walls, and specific experiments were set up to evaluate interactions, initial cell adhesion and cell survivability of *Gram* + & *Gram* – bacteria and yeast. This information about the influence of different factors on the anti-fouling capacity can be potentially extrapolated to different multifunctional coatings for the protection of building materials, allowing to help in the design and optimization of tailored solutions for varying systems and working conditions.

2. Materials and methods

2.1. Synthesis of the nanoparticles and coatings

The AgNPs/N-[3-(Trimethoxysilyl)propyl]ethylenediamine-modified SiO_2 (Ag/N–SiO_2) were synthesized in a three-stage process, according to the methodology reported in previous works [45]. In summary, the process involves: (1) the synthesis of AgNPs from $NaBH_4$ by reduction of $AgNO_3$, (2) functionalization of SiO_2NPs with N-[3-(Trimethoxysilyl)propyl]ethylenediamine (EAPTMS) and (3) grafting of the AgNPs to the functionalized SiO_2NPs via wet deposition, by mixing 1 g SiO_2 with 200 ml of a ~56 ppm AgNPs dispersion (1% nominal Ag content). For comparison purposes, non-functualized particles (Ag/SiO_2) were synthetized by omitting the second step. A detailed description of the process is available in supporting information.

In order to prepare the coatings, the synthesized nanoparticles were incorporated into a hydrophobic formulation based on an ormosil (Organically Modified Silica), synthesized by a sol-gel route (henceforth named BIOC). In addition to the product containing the Ag/N–SiO_2NPs, a product without NPs was synthesized as a control (henceforth referred as HYDRO) to account for the influence of the ormosil matrix over the effectiveness and interactions with the cells. The precursors used for the sol-gel synthesis were a commercial product based on tetraethyl orthosilicate with dioctyltinlaurate as a catalyst (OH100, Wacker Chemie, Germany) and a polydimethylsiloxane with an average chain length of 5 Si–O units and 5% terminal Si–OH groups (PDMS, ABCR, Germany). The starting sols were synthesized according to the general process reported in previous work [45]. The typical synthesis process consists on the following steps: (1) dispersing the particles in a 2% w/v proportion in the silica precursors (86% v/v OH100, 14% v/v PDMS) under an ultrasonic bath for 10 min, (2) adding n-octylamine in a 0.083% v/v proportion (3) sonicating for 10 min at a power of 2 W/cm^3 using a BANDELIN HD 3200 ultrasound probe, with titanium probe model TT25. A detailed description is available in supporting information.

2.2. Application as coatings

The substrates selected for the study were cement mortars, prepared according to EN 196-1 with standardized CEN sand and CEM I 42.5R cement, with a 0.5H_2O/Cement proportions and a 1/3 Cement/Sand ratio. Prismatic 16x4x4 cm^3 blocks were cured for 28 days under 90% RH, cut into 4 × 4 × 2 cm^3 specimens and dried 4 days at 40 °C prior to application of the coatings. Application of the different products was done by brushing following the general process: (1) the sol is applied until apparent saturation (c.a. 0.200 kg/m^2), (2) the product is allowed to absorb for 6 min, (3) a second layer is applied by repeating steps 1 and 2, (4) the excess product is removed with an air gun at 2 bars. After application the specimens were cured and dried under laboratory conditions (20 °C, 45% RH) for 21 days.

2.3. Microorganisms and cell cultures preparation

Five different reference laboratory microorganisms were employed for the bioreceptivity and cell-surface interaction tests, namely: two *Gram* + bacteria (*Bacillus subtilis*, *Staphylococcus aureus*), two *Gram*- bacteria (*Escherichia coli*, *Pseudomonas fluorescens*) and a yeast (*Saccharomyces cerevisiae*). *B. subtilis* (CECT 497), *S. aureus* (CECT 240), *P. fluorescens* (CECT 378) and *E. coli* (CECT 101) strains were acquired from the Spanish Type Culture collection. *S. cerevisiae* strain were isolated from an industrial alcoholic fermentation process and preserved in the culture collection of the Microbiology Laboratory of the Faculty of Marine and Environmental Sciences (University of Cadiz). Fresh bacterial cell cultures were prepared in LB media and incubated for 24 h at 30 °C (for *B. subtilis*, *P. fluorescens* and *S. aureus*) and 37 °C (for *E. coli*). *S. cerevisiae* cultures were prepared in YPD media and incubated at 28 °C for 48 h.

2.4. Characterization techniques

Surface charge of the nanoparticles and microorganisms' surfaces was studied by measuring the zeta potential using a Zetasizer Nano-ZS equipment from Malvern Instruments. Prior to the measurements, the Ag/SiO_2 nanoparticles were dispersed in distilled water (10 mg in 5 ml) and stirred for 10 min in an ultrasonic bath. For determination of the microorganisms' Z-potential, the fresh cultures were diluted in sterile de-ionized water to a concentration of 10^4 CFU/ml.

Contact angles of water and CH_2I_2 were determined through the sessile drop method, employing a video-based, software-controlled contact angle analyzer (OCA 15 plus, Data Physics Instruments). Static contact angles (SCA) were determined using 2.5 μl droplets (5 μl for water CA on the coated mortar surfaces). Water repellence on the coated mortars was determined by the hysteresis between advancing and receding contact angles, measured after adding and removing 2.5 μl to the droplet volume, respectively. Capillary water absorption of the

mortar specimens was measured according to UNE-EN 1925 standard, by placing the surface in contact with water and registering the weight variations over time. Water absorption coefficient was determined as the slope of the ΔM/A (kg/m^2) vs $\sqrt{t}$ (s$^{-1/2}$) curve.

Surface energy of the surfaces and microorganisms, along with their polar and dispersive components, were calculated from the contact angle measurements of two probe liquids, water and CH_2I_2, using the Owens, Wendt, Rabel and Kaelble (OWRK) method [49]. A description of the calculations is available at supporting information. In order to minimize the influence of roughness and porosity over the SCA, the SiO_2NPs samples were prepared by compacting the powder into pellets [50]. Cement mortars samples were prepared by sampling the surface, grinding with a rubber cap, passing through a 100 μm sieve to separate large sand grains and compacting into pellets. The flat hydrophobic coating surfaces were prepared by casting 0.5 ml the sols in flat bottom 12-well microplates and curing for 60 days. The SCA was measured on the surface in contact with the plate. Bacteria and yeast mats for SCA measurements were prepared by collecting the cells on a nylon filter (pore Ø 0.22 μm) to a density of 10^8 CFU/mm^2. To avoid the interference of initial water content [51], the filters were equilibrated at room conditions (20 °C, 40% RH) for 30 min before mounting them into a holder with double-sided tape. The SCA measurements were determined at the initial contact time with the liquid.

Scanning Electron microscopy images (SEM) were registered using a NOVA NanoSEM apparatus (from FEI), in secondary electron mode working at an acceleration voltage of 5.0 kV. The samples were gold sputtered with a 5 nm conductive layer. The SEM specimens colonized with microorganisms were previously fixed in 2% glutaraldehyde solution and dehydrated with successive washes of ethanol/water mixtures (20%, 40%, 60%, 80% and 100%).

2.5. Evaluation of cell-surface interactions

The contribution of electrostatic forces to the interaction of the cells with the NPs was studied by measuring the variations in Z-potential of the cells in the presence of the functionalized (N–SiO_2) or bare SiO_2NPs. The particles without Ag were chosen for the tests to avoid interferences induced by its toxicity. For the tests, 5 ml of the 10^4 CFU/ml cell cultures were mixed with 1.2 mg of the nanoparticles (so that the concentration of the NPs falls below the measurement range) and homogenized in the ultrasonic bath for 1 min. The Z-potential measurements of the microorganisms were performed before and 4 min after the NPs addition.

The contribution of the non-electrostatic forces to the NPs-cell and substrate-cell adhesion was studied by calculating the solid-cell interfacial free energies (ΔF_{adh}) from the polar and dispersive components of their surface energies. For a solid-cell-liquid system, this adhesion energy can be expressed as follows:

$$\Delta F_{adh} = \gamma_{sc} - \gamma_{sl} - \gamma_{cl}$$

Where γ_{sc} is the solid-cell interfacial free energy, γ_{sl} is the solid-liquid interfacial free energy and γ_{cl} is the cell-liquid interfacial free energy. The interfacial free energy between any two phases is calculated from their surface tension components using Good's geometric mean approach:

$$\gamma_{12} = \gamma_1 + \gamma_2 - 2\left[\left(\gamma_1^D\gamma_2^D\right)^{1/2} + \left(\gamma_1^P\gamma_2^P\right)^{1/2}\right]$$

2.6. Biocidal activity of the nanoparticles

The biocide effectiveness of the Ag/SiO_2 nanoparticles against the microorganisms was determined through the plate microdilution method. The assays performed in 96-well plates, adding 50 μl of the NPs dispersions and 100 μl of a 10^6 CFU/ml cell culture, for increasing NPs proportions of 100-10,000 ppm. The negative controls corresponded to wells containing the same NPs concentrations with 100 μl culture media (w/o cells). Positive controls were prepared by adding 50 μl sterile water and 100 μl cell culture. Cell growth was assessed by measuring optical density (OD_{600}) with a ThermoFisher Scientific-Multiskan Go spectrophotometer at the initial time and after 24 h. To avoid setting of the cells/particles, the plate was stirred every 2 h. Cell growth inhibition was calculated according to the following formula:

$$\%\ \text{Inhibition} = 1 - \frac{\left(TF_{Sample} - TO_{Sample}\right) - \left(TF_{CM} - TO_{CM}\right)}{\left(TF_{Growth} - TO_{Growth}\right) - \left(TF_{CM} - TO_{CM}\right)} \cdot 100$$

Where TO_{Sample} and TF_{Sample} correspond to the initial and final values (after 24 h) of each well with the cell culture and particles, TO_{Growth} and TF_{Growth} correspond to the initial and final values of the control w/o NPs, TO_{CM} and TF_{CM} correspond to the initial and final values of controls w/o microorganisms. The EC_{50} values were calculated by regression analysis of the normalized values using Quest Graph™ EC50 Calculator [52].

Susceptibility of the microorganisms to the AgNPs was studied by a semi-quantitative methodology described by Suppi et al. [53]. This methodology was chosen because, in the presence of the culture media, the bare AgNPs experienced a gradual red shift in the SPR band, interfering with the OD_{600} readings. Briefly, fresh cell cultures were prepared at 0.02 OD_{600} and incubated at the optimal temperature for 3 h. Afterwards, the culture media was separated by centrifugation and the pellet was re-suspended in sterile water. 96-well microplates were prepared by adding 100 μl of cell suspension and 100 μl of AgNPs suspension in deionized water to each well (nominal Ag concentrations in the 1–50 ppm range) and incubated at the optimal growth temperature for 24 h. Afterwards, 5 μl of each well were inoculated as a spot in Petri dishes with optimal solid culture medium for growth and incubated for 24 or 48 h. Cell viability was assessed by determining whether growth occurred for each concentration.

2.7. Bioreceptivity assay on mortars

In order to evaluate the effect of the coatings on initial cell attachment and the inhibitory effect of the AgNPs, a methodology from previous works was adapted [45]. This methodology simulates a quasi-static system and prevents gravitational setting of cells on the surface. Specifically, the mortars were placed facing down on a Petri dish containing 15 ml of the cell cultures diluted to 10^6 CFU/ml, covered and gently stirred for 2 h. Afterwards, half of the replicates were sampled with a sterile swab to determine the initial cell attachment and the rest were removed from the plates, flipped upside down and incubated for 24 h (see section 2.4) and subsequently sampled. A set of replicates was also prepared for observation by SEM.

The microbial activity was determined by the chemiluminescence measurement of the total ATP present on the surface with a LUMINULTRA ATP® 2ND GENERATION model luminometer using the Deposit and Surface Analysis kit from the same manufacturer. The relative light unit values were converted to pg (ATP) per area unit by comparison with a reference ATP solution. The fundamentals of the method and calculations are available at supporting information.

3. Results and discussion

3.1. Characterization of the Ag/SiO_2 nanoparticles

The surface properties and size of the nanoparticles, which are exposed to the surface on the superhydrophobic coatings, are among the factors that influence the interaction with the cell walls and, subsequently, the biocide effect of the AgNPs. In relation to these effects, Ag toxicity towards the microorganisms is dependent on the particle size, dispersion and concentration on the carrier SiO_2NPs surface. To account for these factors, a comparative study is presented between the bare and –NH_x functionalized SiO_2NPs.

As detailed in previous studies by the authors [39,45], the size and distribution of the AgNPs over the SiO_2NPs differs depending on the functionalization. The TEM micrographs (available in supporting material, Fig. S1) show that the AgNPs are distributed unevenly over the SiO_2 surface, and a majority of the particles are detached from it. The size of the supported AgNPs is larger compared to the bare AgNPs and large particles (>100 nm) are detected. This effect is attributed to aggregation phenomena during the synthesis process and the low interaction forces with the SiO_2 surface, which is limited to electrostatic interactions. Functionalization of the SiO_2, on the other hand, leads to a homogeneous distribution of the AgNPs over the N–SiO_2 surface and their size is similar to the bare AgNPs. This is attributed to the strong interactions of the surface –NH_x groups with the Ag surface through ligand-metal bonds. Further evidence of the interactions is found on the yield of the deposition process (Table 1), which increases from 67% to 92% (nominal Ag content was set to 1%) for the functionalized SiO_2.

Surface charge, estimated through the Z-potential values (Table 1), determines the contribution of electrostatic interactions with the cell walls—generally possessing a negative charge—that influence attachment stages and the contact with the biocide. Bare SiO_2 particles display a negative Z-potential, which is consistent with the acid character of the Si–OH groups on their surface (pH of the NPs dispersion was <4). After functionalization, the Z-potential of the N–SiO_2NPs becomes positive due to the basic character of the –NH_x groups, that possess a positive charge density and/or positive charge in their protonated form. Deposition of AgNPs over the bare SiO_2 barely modifies the magnitude of the charge, whereas a decrease was observed for the functionalized N–SiO_2NPs (albeit the charge was still positive). Considering that the bare AgNPs show a positive charge due to lactam groups of the capping/stabilizing agent (PVP), this can be directly related to blocking of the –NH_x groups by the AgNPs.

To account for non-specific interactions other than electrostatic forces (e.g. Dipole-dipole, London dispersion), the polar and dispersive components of the SiO_2NPs surface energy were determined (Table 2). The bare SiO_2NPs present a relatively high surface energy, mainly represented by their polar component. This high polarity may be attributed to the silanol groups on their surface. The functionalized N–SiO_2NPS showed a similar dispersive surface energy, and the polar component only decreased slightly, likely due to the lower polarity of –N-H bonds compared to –O-H.

3.2. Characterization of the coating and mortar surfaces

Bacterial adhesion on a material is a complex process that depends on multiple factors [32], including but not limited to surface-cell interaction forces, surface roughness and topography or wetting properties. Along with the initial attachment, water retention inside the material promotes biofilm growth.

The surface energy of the materials conforming the substrate and coatings is presented in Table 2. For the mortar, the surface energy was determined on two systems, representative of the components exposed on the surface: (1) the cementitious matrix (referred as cement), mainly composed by the cement hydration products (portlandite, calcium silicate hydrate, ettringite …). (2) Quartz, which is the main component of the sand. The cementitious matrix shows a relatively high surface energy

Table 1
Properties of the Ag and SiO_2–Ag nanoparticles used in this study.

	Size (Ag)/nm	% Ag[a]/%wt.	Z-potential/mV
Ag	11.8 ± 3.6	n/a	9.8 ± 0.4
SiO_2	n/a	n/a	−27.6 ± 0.4
N–SiO_2	n/a	n/a	45.5 ± 1.3
Ag/SiO_2	15.0 ± 6.1	0.67 ± 0.05	−24.7 ± 0.4
Ag/N–SiO_2	9.2 ± 3.2	0.92 ± 0.02	30.7 ± 0.4

[a] Determined by ICP-AES. Nominal content 1%.

Table 2
Surface energy and its polar and dispersive components of the material surfaces, calculated by OWRK method.

	γ^D/erg·cm^{-2}	γ^P/erg·cm^{-2}	γ/erg·cm^{-2}	[c]Polarity/%
SiO_2	17.8	52.8	70.6	75
N–SiO_2	17.7	47.3	65.0	73
[a]Cement	27.2	41.9	69.1	61
[b]Quartz	36.8	22.2	59.0	38
HYDRO	30.4	2.8	33.2	8
BIOC	36.4	0.7	37.1	2

[a] Corresponding to the mortar cementitious matrix.
[b] Corresponding to the sand used in the mortar preparation.
[c] Calculated as γ^P/γ *100.

with a major contribution of the polar component, owing to the presence of polar groups (e.g. Si–OH, Al–OH, hydration H_2O molecules) and/or trapped ions (e.g. Ca^{2+}). The γ value for quartz is lower, and its dispersive component is more significant. On the other hand, the HYDRO and BIOCIDE gels, representative of the coatings, have a lower surface energy with a minimal contribution of the polar component. This is characteristic of the presence of aliphatic alkyl chains in the xerogel structure, formed by co-polymerization of the alkylsiloxanes, alkylalkoxysilanes and TEOS. By comparing the HYDRO and BIOC surfaces, a slight increase is observed in the γ values of the latter, attributable to the presence of the N–SiO_2NPs. Anyways, the differences are of little relevance and the effects of surface roughness on the measurements cannot be fully discarded.

Changes on surface topography after application of the coatings, down to the sub-micron scale, are presented in the SEM micrographs (Fig. 1). The untreated mortar surface (Fig. 1A–C) is characterized by an irregular roughness at the micrometric scale, where typical morphologies of cementing phases are visible (portlandite hexagonal plates, ettringite needles, foil-like C–S–H). After treatment with HYDRO (Fig. 1D–F), the surface presents a slightly more compact aspect, specially in the micrometric range, where the polymerization products are partially covering the features observed on the untreated mortar. At higher magnification, the coating presents irregular or poorly defined foil-like structures, which are consistent, respectively, with the formation of organically modified silica by auto-condensation and C–S–H gel by reaction with the cement matrix [54]. In a similar vein to the untreated mortar, no regular patterns are observed in the surface morphology. The surface treated with BIOC presents more marked differences due to the presence of the Ag/N–SiO_2NPS (Fig. 1G–H). As evidenced by the micrographs, the particles accumulate on the surface, creating a compact layer that covers the topographical features and leads to a flatter profile at the micrometric range. At higher magnifications, though, it can be observed that the (50–100 nm) particles are arranged in such a way that the surface presents a high nano-roughness characterized by regularly spaced peaks.

Wetting properties of the surfaces (Table 3), which depend on their roughness and surface energy, influence the water absorption capacity and the adhesion of microorganisms or extracellular matrix components to the surface, all of them factors involved in the different stages of biofilm formation. The untreated mortar, in line with its high surface energy, behaves as a hydrophilic material, with static contact angles below 30° (it should be noted that accurate measurements are difficult to the quick absorption). After treatment with the HYDRO coating, the surface shows a marked hydrophobic character with a SCA of 141°. The low surface energy of the coating (~30 erg cm^{-2}) by itself does not suffice to explain such high values, as typical SCA values on ormosils range in the 90–110°. As observed in the SEM micrographs (Fig. 1), the HYDRO surface shows a rough aspect with disordered features at the micron and sub-micron scale, which contribute to an increase in the apparent contact angle according to the Wenzel wetting model [55]. Specifically, the Wenzel model states that, for a surface with a random roughness, the static contact angle is proportional to the extended

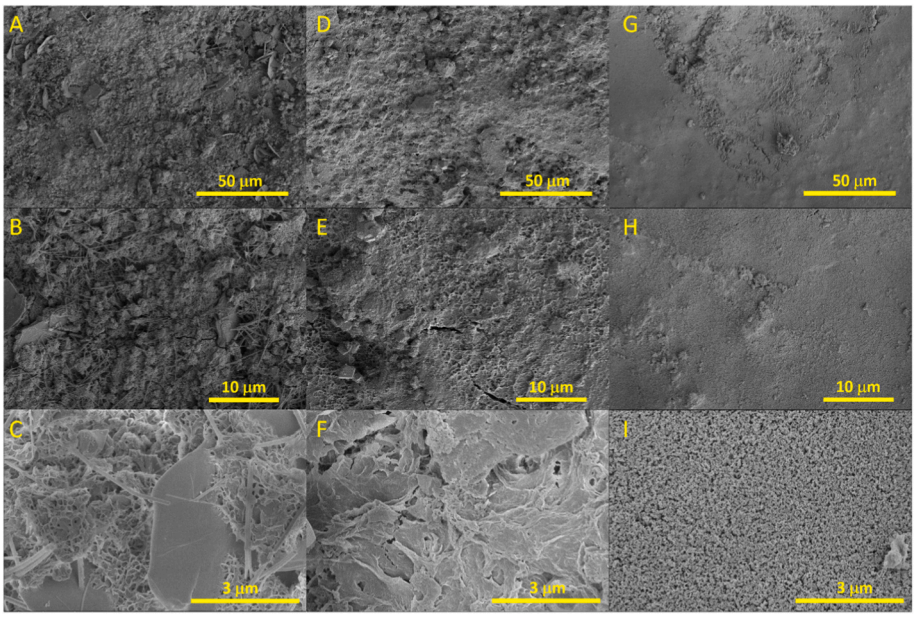

Fig. 1. SEM micrographs of the mortar surfaces. (A–C) Untreated. (D–F) Treated with HYDRO. (G–I) Treated with BIOC.

Table 3
Wetting properties (static contact angle and hysteresis), capillary water absorption coefficient and total water absorption after 48 h of the mortars.

	SCA/°	Hysteresis/°	WAC/kg·m^{-2}·s$^{-1/2}$	TWU/%w
Untreated	≤30	n/a	0.030	3.4
HYDRO	141 ± 4	15 ± 1	0.005	0.6
BIOC	153 ± 2	7 ± 1	0.001	0.2

area/projected area ratio. Another characteristic of a Wenzel surface, observed for the HYDRO surface, is the pinning of the water droplets, as they fully impregnate the roughness features, which is evidenced by relatively high contact angle hysteresis (>10°). The BIOC surface, on the other hand, is characterized by a superhydrophobic behavior (SCA >150°, Hysteresis <10°), which, considering its similar surface energy respect HYDRO, can be attributed to the promotion of a Cassie-Baxter wetting regime due to its surface topography [56]. The presence of regularly spaced roughness features at the nanometric scale promotes the entrapment of air pockets between the surface and water, decreasing the interaction forces (which explains the water repellence phenomena) and increasing the contact angle proportionally to the amount of entrapped air.

Different authors have reported that the low interaction of superhydrophobic surfaces with aqueous systems and polar substances is an effective route to decrease cell deposition and/or facilitate the detachment of biofilms [34,36,57,58] by cleaning actions, as a combination of the high contribution of the air-solid interface and the presence of roughness valleys smaller than the cell dimensions [31,59]. However, the superhydrophobic surfaces may be ineffective and even increase cell attachment under favorable circumstances [32,36]. Examples of factors causing this behavior include: (1) Contamination of the surface causes it to transition to a Wenzel state, which implies an increase of the effective contact area. (2) Non-polar substances—including some of the cell wall components—may attach more strongly to hydrophobic surfaces. (3) The effect of the roughness valleys on cell attachment is dependent on their morphology, size range (e.g. its relevance decreases at smaller sizes) and the rigidity of the cell walls.

Aside from surface phenomena, water absorption capacity of the materials is related with their bioreceptivity, as water availability is essential for microbial growth. This factor is the main reason why hydrophobic or waterproof coatings are commonly used to control the growth of molds and algae on building materials susceptible to dampness. The capillary absorption coefficient and total water absorption (Table 3), calculated from the absorption curves (see Fig. S2 in supporting material), of the mortars before and after treatment evidence a clear decrease due to the hydrophobic character of the coatings, with reductions in the 80–95% range. This mostly results from the low surface energy of the coated pore walls, which significantly decreases the capillary suction forces [60]. The slightly lower absorption of the mortar treated with BIOC respect HYDRO is likely because the compact nano-SiO_2 coating partially covers the surface pores.

3.3. Study of cell-surface interactions

Biofilm formation and biofouling processes involve multiple stages which depend on different factors related to the environment, the materials and the specific microorganisms [32]. These processes become even more complex when the changes in the system over time are considered. Regardless of this, the initial stages of biofilm formation are essential to the progress of the process. Specifically, the first stage involves the attachment of the cells (generally bacteria) to the surface via non-specific attraction forces with the cell walls (electrostatic, Van de Waals) and/or specific interactions [32], with the former depending exclusively on the physical-chemical properties of the substrate and the cell walls.

In order to study the influence of electrostatic forces, the Z-potential of the microorganisms was measured and its variation, after contact with the non-functionalized (negative charge) and functionalized (positive charge) SiO_2 particles, was determined (Fig. 2A–B). In accordance with other studies found in literature [61,62], all the microorganisms present negative Z-potential values due to the charge densities of their outer wall components. More specifically, this charge is influenced by the presence of negatively charged peptidoglycan in the case of *Gram* + and *Gram* – bacteria [61], lipopolysaccharides in the case of *Gram* – bacteria, and β-glycan, chitin and mannoproteins in the case of the yeast [62]. The differences between microorganisms depend on multiple factors, including the strain and metabolic state, that affect the structure and composition of the external cell walls. The more negative value observed for *E. coli* is consistent with data reported by other authors [63] and may be related to the negative charge density of the lipopolysaccharide layer.

The interaction with the SiO_2NPs causes in all cases changes of the

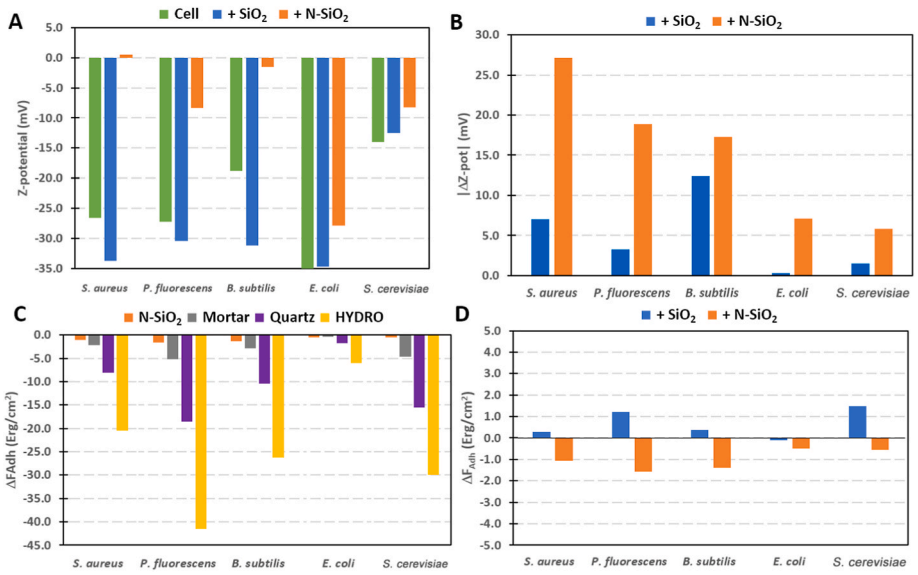

Fig. 2. Study of the cell-surface interactions. (A) Z-potential of the microorganisms before and after contact with the SiO_2 nanoparticles. (B) Variations of Z-potential expressed as absolute value. (C) Surface-cell adhesion forces in aqueous system, calculated from the interfacial energies balance. (D) Surface-cell adhesion forces calculated for the functionalized and bare SiO_2 nanoparticles.

cells' Z-potential, which are indicative of the interactions, and the influence of the particle surface charge becomes evident by the consistently higher magnitude of these variations with the positively charged N–SiO_2NPs. On the one hand, the Z-potential of the cells experiences relatively low changes towards negative values after contact with the bare SiO_2, which are expected considering the electrostatic repulsion should hinder the particle-cell contact. On the other hand, the positive charge of the N–SiO_2NPs generates an electrostatic attraction, which may explain the overall variations of Z-potential over four times higher in comparison with the bare SiO_2NPs. In the case of *B. subtilis*, the trend is maintained but the differences between particles are less marked. Although *B. subtilis* is coincidentally the organism with a lower surface charge, this factor alone would not suffice to explain the observed behavior, as the differences for *E. coli* were not the highest despite it having the more negative charge. Considering that the differences in surface energy between the particles (Table 2) and non-specific cell-surface adhesion forces (Fig. 2D) are subtle, it can be assumed that the observed behavior is governed by both electrostatic and specific interactions with the surface Si–OH and –NH_x groups.

The obtained results are in line with a previous work from the authors [39], where it was observed through Z-potential measurements that the electrostatic interaction of the particles with algae and cyanobacteria significantly increased for the –NH_x functionalized SiO_2 particles. In the aforementioned work, a more evident effect of the microorganism surface charge was observed, though it should be considered that their differences were more marked and one of the organisms possessed domains with positive charge. Other authors have also observed [37] a marked difference in bacterial cell adhesion to gold surfaces functionalized with positively charged –NH_2 and negatively charged –COOH groups respectively, and the attributed the adhesion kinetics to the former to a diffusion-controlled process with no activation energy or with values below the thermal energy. Overall, the electrostatic charge of the surfaces has been consistently reported by different researchers as a factor with a high influence on microbial adhesion [32].

Other than electrostatic interactions, the non-specific attraction forces (e.g. London, dipole-dipole) may play an important role on the initial cell attachment, although their effect is not as straightforward and there are conflicting reports in scientific literature [32], since it also depends on the environment (i.e. medium composition, flow conditions …) and it is difficult to isolate them from other factors under experimental conditions. In a simplified manner (assuming no specific interactions), it is possible to estimate the work of adhesion of a cell to a surface through the balance of interfacial tensions in the cell wall-surface-water (medium) system, which ultimately depends on the non-specific polar and dispersive forces. A lower (more negative) work of adhesion indicates that the formation of the cell wall-surface interface is thermodynamically favorable. For the present work, the work of adhesion was calculated, using Good's geometric mean approach, from the polar and dispersive surface energy components of the materials (Table 2) and microorganisms (Table 4). The calculations considered adhesion in an aqueous system ($\gamma^P = 51.0$ erg cm^{-2}, $\gamma^D = 21.8$ erg cm^{-2}), as all bioreceptivity and biocidal tests were performed in diluted culture media with similar surface tensions.

By comparing the work of adhesion (ΔF_{Adh}) calculated for the bare and functionalized SiO_2NPs (Fig. 2D), it can be observed that the interaction with the cells is disfavored for the former (except for *E. coli*), and the functionalization slightly increases the adhesion. In any case, the values for the work of adhesion are low and the differences do not reach ±2.5 erg cm^{-2} for neither of the microorganisms, suggesting that these non-specific interactions do not play a significant role in the Z-potential changes from the experiment described previously (Fig. 2A). Regarding the trends, it can be observed that adhesion to the bare SiO_2 is favored for the microorganisms with a higher contribution to the polar component, whereas the trend is inverted for the N–SiO_2NPs, which coincidentally become slightly less polar after functionalization.

The differences in ΔF_{Adh} become more pronounced when comparing the other surfaces relevant for this study (Fig. 2C), namely: the cement mortar (matrix), quartz (aggregate) and the HYDRO xerogel (coating).

Table 4
Surface energy and its polar and dispersive components of the microorganisms' surfaces, calculated by OWRK method.

	γ^D/erg·cm^{-2}	γ^P/erg·cm^{-2}	γ/erg·cm^{-2}	[a]Polarity/%
E. coli	19.5	44.2	63.6	*69.4*
P. fluorescens	25.3	12.4	37.7	*32.9*
B. subtilis	19.9	23.9	43.9	*54.6*
S. aureus	20.3	29.1	49.4	*58.9*
S. cerevisiae	31.3	20.0	51.3	*39.0*

[a] Calculated as γ^P/γ *100.

For all microorganisms, the magnitude of ΔF_{Adh} is the lowest on the N–SiO_2, which is expected considering their surface energy and polarity are close to water, minimizing the cell wall-media interface tensions. The adhesion becomes more favorable as the substrate surface tension and polarity decrease in the order mortar < quartz ≪ HYDRO. In fact, the differences increase for the microorganisms with a lower polarity up to the point that the absolute values of ΔF_{Adh} on the HYDRO surface are one order of magnitude higher than on mortar for *P. fluorescens* and *S. cerevisiae*. In the case of *E. coli*, which has the highest polarity and surface energy, the trend is maintained but differences are less remarkable.

This higher adhesion of the microorganisms to the hydrophobic surfaces is in line with previous works from the authors [39], where it was also determined that the effect of the hydrophobic surface was more marked for cyanobacteria species with a low polarity (*Synechococcus* sp.) compared with those containing highly polar cell wall components (*Phormidium* sp.). Oh et al. [37] also found in their experiments that a decrease in surface energy of coated surfaces with controlled chemistry increased the number of attached *E. coli* and *S. aureus* cells, which they attributed to a higher contribution of the Van der Waals forces decreasing the total energy of the system.

To have a better understanding of the trends observed for the work of adhesion, it is necessary to define the different interfacial tensions involved in the cell wall-substrate-media triple interface and how the material and cell composition affect them. The interfacial tension ($\gamma_{A\text{-}B}$) defines the free energy involved in increasing the contact area between two phases A and B, meaning that lower interfacial tensions are more favorable. Attachment of a cell on a substrate—assuming monolayers and disregarding cell-cell interactions, as we are considering only the initial stage of biofilm formation—involves an increase of the cell-substrate contact area (defined by $\gamma_{C\text{-}S}$) and an equivalent decrease of the cell-water ($\gamma_{C\text{-}L}$) and substrate-water ($\gamma_{S\text{-}L}$) areas. Fig. 3 shows the

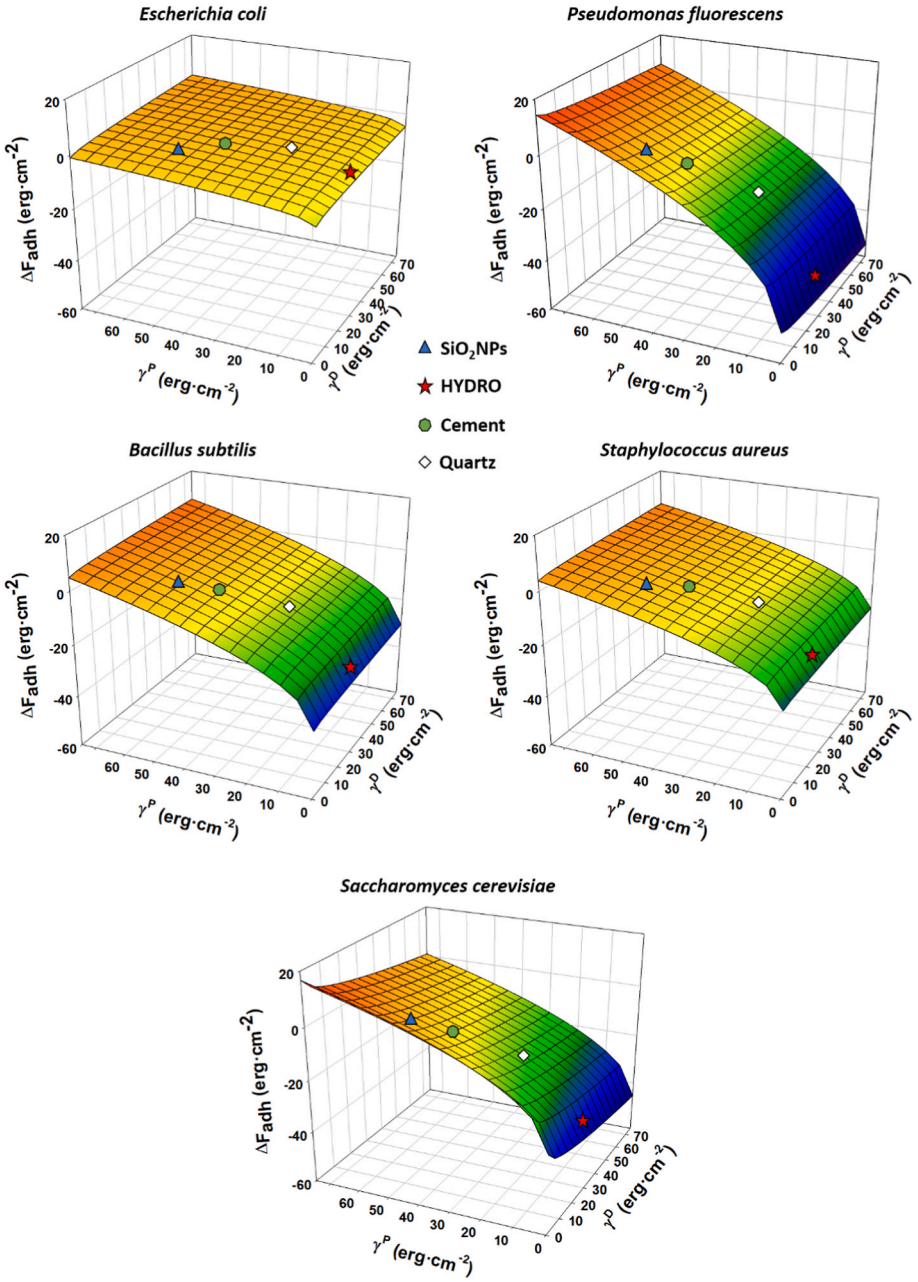

Fig. 3. Estimation of the cell-surface adhesion forces, in an aqueous system, varying the polar and dispersive components of the surface energy. The dots represent the surfaces tested in this study.

variations of the work of adhesion—calculated from the surface energies balance—for each microorganism with the polar and dispersive components of the substrate surface energy. For all cases, adhesion is disfavored at higher values of the polar component of the substrate, whereas the influence of its dispersive component is comparatively lower and it depends on the polarity of the microorganism surface (i.e. its increase favors cell adhesion for *S. cerevisiae* and *P. fluorescens*, organisms with the least polar contribution).

Independently from the microorganism, one of the factors that favors cell adhesion to the hydrophobic surfaces (i.e. HYDRO) is the relatively high energy of the surface-water interface, as, in contrast with water, these are characterized by a low surface tension with a major contribution of the dispersive component (Table 2). As a consequence, reducing the water-substrate contact area on surfaces such as HYDRO, whose $\gamma_{S\text{-}L}$ values are $\geq$30 erg cm^{-2}, would contribute to decreasing the energy of the system. The opposite holds true for hydrophilic surfaces with a distribution of their polar and dispersive components similar to water, such as the mortar and silica with $\gamma_{S\text{-}L}$ values $\leq$ 5 erg cm^{-2}.

On the other hand, the contribution of the cell wall-water interface highly varies for the different microorganisms. In general, the $\gamma_{C\text{-}L}$ values (Table 5) follow an inverse trend to the polarity, rather than the total surface energy of the cell wall, with the minimum found for *E. coli* ($\gamma_{C\text{-}L}$ = 0.3 erg cm^{-2}) and the maximum for *P. fluorescens* ($\gamma_{C\text{-}L}$ = 13.2 erg cm^{-2}). In other words, the decrease of the cell-water interface area will contribute favorably to the adhesion on a surface for those organisms with a less polar cell wall.

The cell wall-substrate interface generally has a higher influence than the cell-water one, and the differences in interfacial tensions vary heavily with the microorganisms. In the case *P. fluorescens*, the interfacial tension ($\gamma_{C\text{-}S}$) is lower for the hydrophobic surface (HYDRO) respect to the hydrophilic phases (mortar, silica), and the differences between substrates with varying surface energies are more marked due to the low polarity of the cell's surface. This higher stability of the cell-substrate interface, along with the high cell-water surface energy explains why the highest adhesion on hydrophobic surfaces is calculated for this microorganism. For the rest of the microorganisms, the $\gamma_{C\text{-}S}$ values are actually higher on the HYDRO surface, although the differences respect to the hydrophilic substrates are relatively low (~5–13 erg cm^{-2}) except for *E. coli*. Therefore, the higher energy of the cell-substrate interface on a hydrophobic material is offset by the decrease in the total energy promoted by the reduction in the substrate-water ($\gamma_{S\text{-}L} \geq$ 30 erg cm^{-2}) and, to a lesser extent, cell-water ($\gamma_{C\text{-}W}$ ~3–8 erg cm^{-2}) contact areas. On the other hand, the differences in substrate-cell surface energy for *E. coli* with hydrophobic or hydrophilic substrates are in a similar range (20–25 erg cm^{-2}) to the substrate-water interface, and its cell-water interface energy has a low contribution (0.3 erg cm^{-2}) due to the cell's high polarity. In this case, the energies of the substrate-water and substrate-cell interfaces practically compensate each other, leading to a lower influence of this factor over the initial adhesion.

It is worth mentioning that the considerations based on surface energy balances are mostly representative of the initial stages of cell attachment and do not take into account specific interactions, heterogeneities of the cell wall nor the influence of elastic deformation forces [37]. At longer time scales, other factors may modify the involved surfaces or the attachment processes, including but not limited to: (1) The secretion of extracellular substances (EPS) and their adsorption on the substrate can alter its surface energy and charge, as well as promote specific interactions with the cells and formation of clusters [64]. (2) At high cell densities, the bacteria may be able to produce and release chemical signals that regulate gene expression, affecting key processes in biofouling such as EPS secretion, motility or cell division [65]. (3) Certain motile bacterial species, including *E. coli*, possess chemotaxis mechanisms [65] that allows them to detect and respond to chemical gradients through specific receptors. Specifically, it has been found that *E. coli* produces exopolysaccharides, which promote the formation of bacterial clusters.

Table 5
Surface tension values calculated for the cell-water and cell-solid interfaces.

	$\gamma_{C\text{-}L}$ (water)/ erg·cm^{-2}	$\gamma_{C\text{-}S}$ (mortar)/ erg·cm^{-2}	$\gamma_{C\text{-}S}$ (HYDRO)/ erg·cm^{-2}	$\gamma_{C\text{-}S}$ (quartz)/ erg·cm^{-2}	$\gamma_{C\text{-}S}$ (N⁻SiO2)/ erg·cm^{-2}
E. coli	0.3	0.7	25.9	6.5	0.1
P. fluorescens	13.2	8.7	3.7	2.5	14.7
B. subtilis	5.1	2.6	11.5	3.1	4.0
S. aureus	3.1	1.7	14.9	2.9	2.3
S. cerevisiae	8.0	4.1	7.8	0.3	7.7

3.4. Biocidal activity of the nanoparticles

The susceptibility of the different microorganisms to the toxic effects of the active biocide agent is, along with the adhesion properties, one of the factors that determine the antimicrobial effect of the coatings. As noted by different authors [47,48], the biocide effectiveness of nanoparticles depends not only on the release of soluble species (e.g. Ag^+) to the media, which is governed by their size and composition, but also on their ability to interact with the cell surface promoting contact mechanisms and localized release of toxic ions. This interaction capacity is ultimately determined by the adhesion forces (e.g. electrostatic, dipole-dipole, London …) and the specific area of the particles or their clusters.

In order to check the susceptibility of the tested microorganisms towards Ag without interference from the carrier SiO_2NPs surface properties and aggregation processes, a semi-quantitative spot test [53] was performed (Table 6).

In all cases, it was observed that the minimum inhibitory concentration (MIC) of the AgNPs, falls below 10 ppm, demonstrating that the active component is expected to present toxic effect in the concentration range used for the coatings (c.a. 200 ppm in the BIOC sol). *P. fluorescens* and *S. cerevisiae* were the most sensitive species, showing total growth inhibition at 1 ppm Ag, whereas growth was partially inhibited at 1–5 ppm for *E. coli*, *S. aureus* and *B. subtilis*. Silver nanoparticles have been generally found less toxic to *Gram* + bacteria than *Gram* - [48], which is in line with the obtained results. The higher resistance of *Gram* + bacteria has been attributed to the thicker peptidoglycan layer of their outer wall (20–80 nm), which protects against physical damages by the particles and hinders the uptake of Ag^+ ions. On the other hand, the lipopolysaccharide layer on the outer wall of *Gram* – bacteria possess negatively charged domains that can increase the uptake and accumulation of released Ag^+ ions.

Toxicity of the silver supported over the carrier SiO_2 follows a different trend, manifesting the influence of surface phenomena and particle aggregation. The dose response curves (Fig. 4) and the obtained EC50 values (see Fig. 5B for values normalized for Ag concentration) fall in ranges consistent with the spot test, with inhibitions of 35–70% in the 100–500 ppm Ag/SiO_2 (c.a. 1–5 ppm Ag) and values in the 75–80% at higher concentrations, where the spot test showed total growth inhibition. Overall, the spot test showed a higher activity of the bare AgNPs at

Table 6
Susceptibility of the microorganisms towards the AgNPs, according to the "spot test". (-) Total inhibition. (+-) Partial inhibition/biostatic effect. (++) Normal growth.

	E. coli	P. fluorescens	S. aureus	B. subtilis	S. cerevisiae
50 ppm	-	-	-	-	-
40 ppm	-	-	-	-	-
30 ppm	-	-	-	-	-
20 ppm	-	-	-	-	-
10 ppm	-	-	-	-	-
5 ppm	+-	-	+-	+-	-
1 ppm	+-	-	+-	+-	-
Control	++	++	++	++	++

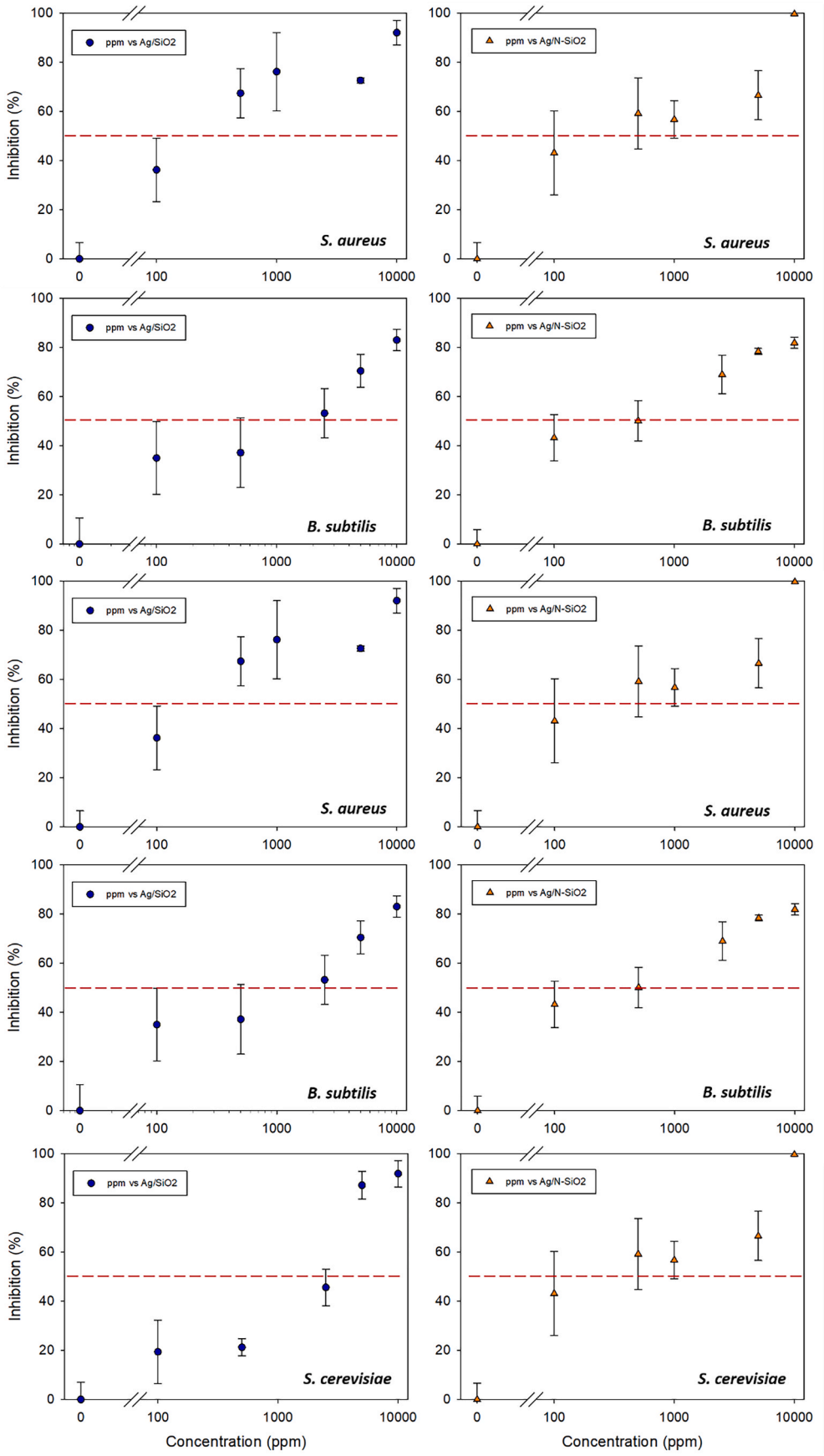

Fig. 4. Dose-response curve obtained from the micro-dilution test results for the bare and functionalized Ag/SiO_2NPs.

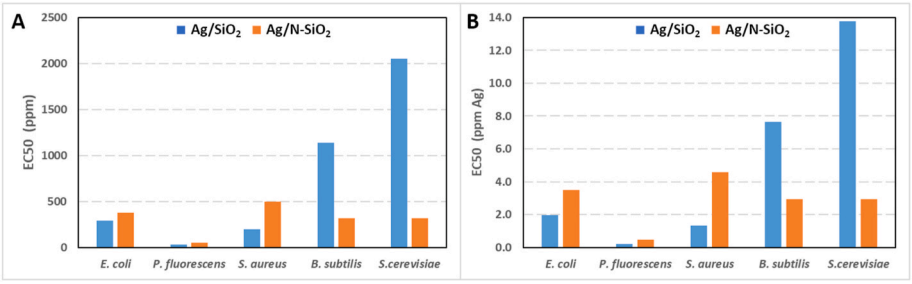

Fig. 5. (A) EC50 values of the bare and functionalized Ag/SiO_2NPs calculated from the dose-response curves. (B) EC50 values expressed as a function of Ag concentration.

lower concentrations, which can be attributed to their lower tendency to aggregate and the differences in the experimental setup (e.g. some components of the liquid media in the micro-dilution test contain –NH_x and –SH moieties that can interfere with AgNPs). It should be noted that, at high Ag/SiO_2 concentrations, OD_{600} values are less precise due to turbidity of the media. In both tests, inhibition was the highest for *P. fluorescens*, indicating that its susceptibility is the predominant factor. *S. cerevisiae*, on the contrary, showed a lower susceptibility to Ag/SiO_2.

Toxicity of the functionalized particles (Ag/N–SiO_2) with positive charge was, in most cases, similar or higher than the negatively charged Ag/SiO_2 (see EC50 values in Fig. 5). For *E. coli* and *P. fluorescens*, the differences are of little significance, suggesting that the effect of the Ag is predominant over the SiO_2 surface under the test conditions. Surface charge, however, played a more relevant role in the tests for *B. subtilis* and *S. cerevisiae*, decreasing EC50 by a factor of 4–5 for the N–SiO_2 with positive charge. As pointed out by different researchers [45,47,48], a positive electrostatic charge can enhance the contact of the biocides with the cell walls, which is in line with the Z-potential measurements (Fig. 2A), and increase their effectiveness. While this phenomenon likely occurs under our experimental conditions, the differences in EC50 do not follow the same trend as those in electrostatic interactions, even showing a lower effect for Ag/N–SiO_2 in the case of *S. aureus*. The differences in non-specific forces of adhesion (Fig. 2D), on the other hand, are too small to justify these differences. Thus, it can be assumed that other unaccounted for factors are affecting the results, namely: (1) the functionalization process of the Ag/N–SiO_2 particles makes them more susceptible to aggregation phenomena, as reported in works using similar synthesis processes for Ag/TiO_2 systems [66]. This leads to a lower effective area and subsequent decrease in toxicity. (2) The different microorganisms may possess specific interaction mechanisms with the particles surface, especially in the case of N–SiO_2 which has –NH_x groups, similarly to common biomolecules.

3.5. Bioreceptivity of the mortars

Bioreceptivity of the mortar surfaces and the capacity of the biocide to inhibit cell growth were evaluated through the ATP measurements on the surfaces at short times after inoculation and after incubation for 24 h. Under the test conditions, the effect of gravitational setting is minimized, and the ATP signal (proxy for the number of cells) at 2 h is representative of the initial cell attachment on the surface. These interactions are complex and depend on the magnitude of the interactions, partially determined by electrostatic charge and surface energies of the cell all and material surface, and factors related to surface topography

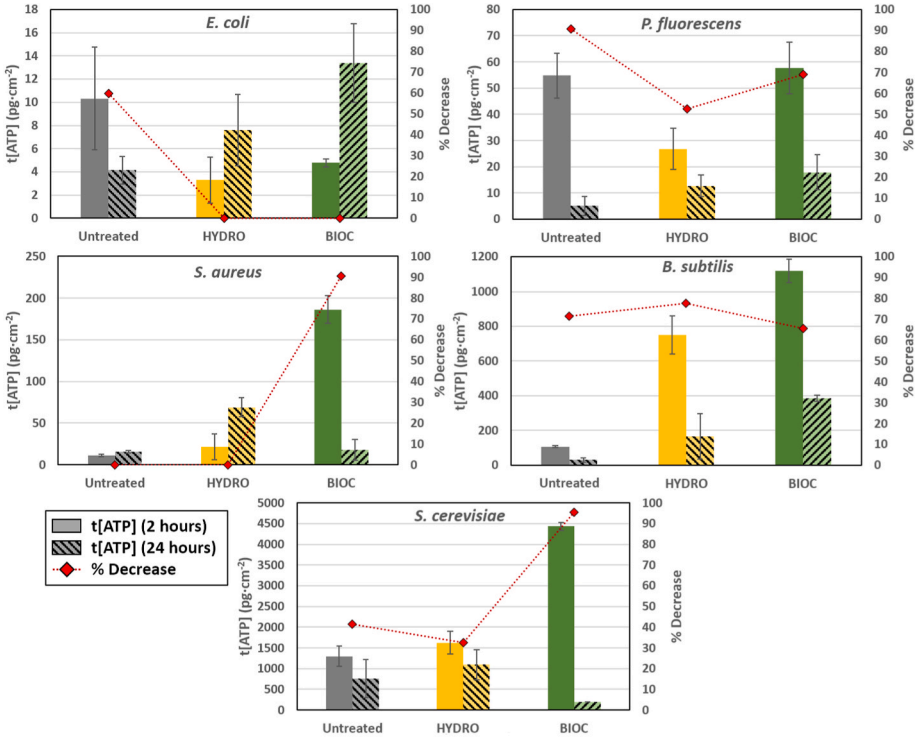

Fig. 6. Results from the bioreceptivity test on the untreated and treated mortars. %Decrease corresponds to the different between t[ATP] at 2 h and 24 h.

(e.g. roughness, morphology, surface pores) [32,67].

The ATP measurements at 2 h for the different the microorganisms (Fig. 6) show a number of general trends that can be related to the characterization data and cell properties. When comparing the untreated mortars with those coated with the hydrophobic primer (HYDRO), different behavior is displayed by the *Gram* – (*E. coli* and *P. fluorescens*) and *Gram* + (*S. aureus* and *B. subtilis*) bacteria. The *Gram* – bacteria showed a lower adhesion to the hydrophobic surface, whereas the *Gram* + bacteria attached more strongly, especially in the case of *B. subtilis*. The yeast *S. cerevisiae* displayed a similar trend to the *Gram* + bacteria. As predicted from the interfacial tension calculations (Figs. 3 and 2C), the force of adhesion by non-specific interactions is in all cases higher for the hydrophobic coating than the hydrophilic substrate (composed by quartz and cement matrix). On the other hand, the effect of the coating on other surface properties may contribute to decrease cell adhesion and offset the adhesion forces. More specifically, (1) the SEM micrographs (Fig. 1) evidence a decrease in micrometric roughness features after coating with HYDRO. Multiple studies have demonstrated that rough surfaces in the micron scale (similar to the cell size) promote cell adhesion due to their higher specific area. (2) Surface charge of the mortars at neutral and basic pH is generally positive [68,69] due to the adsorption of Ca^{2+} ions, whereas the HYDRO coating forms a silica gel (ormosil) which typically has negative charge due to the acidic Si–OH groups on its surface.

In the case of *E. coli*, the influence of surface energy over cell adhesion is the lowest (Fig. 3), which may explain why the other opposing factors are predominant. The behavior of *P. fluorescens*, however, is contradictory with the adhesion force calculations and, while the test with the SiO_2 particles showed a high influence of electrostatic forces over the surface-cell interactions (Fig. 2A), this factor alone would not suffice to explain the differences. Thus, the results suggest that adhesion of *Gram* – bacteria seems more influenced by specific interaction mechanisms. As an example, some authors [32] have identified the role of fimbria/pilli on the early stages of biofilm formation, which promote the interaction between cells (manifesting in cluster formations) and certain abiotic surfaces. Similarly, cell motility and properties of the flagella have been identified by some authors as relevant factors. Adhesion of the tested *Gram* + bacteria seems to be mostly influenced by the non-specific adhesion forces, as the trend of the ATP values matches the calculated forces (Fig. 3), where the higher adhesion is observed on the hydrophobic surfaces and the differences with the untreated mortar become more marked for *B. subtilis*. Anyways, deeper characterization studies would be required to discern the effect of cell-specific mechanisms from physical interaction forces.

By comparing the ATP measurements on the HYDRO and the BIOC surfaces, a clear increase of cell adhesion on the latter is observed for all the microorganisms despite its superhydrophobic character. The antifouling capacities of superhydrophobic surfaces have been studied by different authors [34,36,57,58], as their low interaction with aqueous systems (i.e. Cassie-Baxter state), self-cleaning effect, and topographical details smaller than cell size can hinder cell adhesion and facilitate biofilm removal under flow conditions. However, the first two effects are lost when the surface switches from a Cassie-Baxter to a Wenzel state, which is a common effect of contamination with organic matter (e.g. EPS, atmospheric pollutants), and the increased roughness can increase cell adhesion if their wall is sufficiently flexible.

Under the experimental conditions used in this study, a number of factors may contribute to the higher adhesion on the superhydrophobic surface, namely: (1) the experimental measurements showed that the surfaces after inoculation switch to a Wenzel state (SCA $\approx$ 120°, H $\approx$ 20°). Under these conditions, the effective contact area is increased due to their high nano-roughness, promoting cell adhesion due to their high affinity for the hydrophobic surfaces (see Fig. 3). (2) The BIOC coating contains positively charged N–SiO_2NPs exposed on the surface (Fig. 1) that promote cell adhesion through electrostatic attraction, as evidenced by the Z-potential experiments (Fig. 2A and B). (3) The experimental setup simulates static/low flow conditions, which are more representative of the working conditions of building elements exposed to the environment.

An evidence suggesting the influence of the N–SiO_2 positive charge is found when comparing the differences between bacterial adhesion on HYDRO and BIOC. Specifically, this difference is more marked for *P. fluorescens* and *S. aureus*, which coincidentally are the bacteria that showed a higher shift in Z-potential after contact with the N–SiO_2NPs (see Fig. 2A and B). In a similar vein, the difference in adhesion is lower for *E. coli*, which showed the lowest sensitiveness to the particle charge and surface hydrophobicity (Fig. 3), suggesting that the increase in roughness may have a lower effect. Another factor that may influence the initial adhesion results is cell motility, as suggested by the remarkably higher increase in adhesion observed for *S. aureus* and *S. cerevisiae*, which are both non-motile organisms. In the case of the yeast, this aspect may explain in part why the differences are high despite a comparatively low influence of the N–SiO_2NPs electrostatic charge. The effects of cell motility on adhesion to abiotic surfaces have been studied by different authors [32], who suggest some organisms take advantage of chemotaxis mechanisms to move away from unfavorable surfaces or counter weaker physical adhesion forces. Identifying if such effects occur in the test conditions of this work, however, would require deeper studies (e.g. comparison with mutant strains w/o functional flagella).

The ATP measurements after incubation for 24 h evidence how survival of the microorganisms was affected by the substrate and coating composition, which, along with the differences in initial number of attached cells can even mask the effect of the biocide agent (Ag/N–SiO_2). With the exception of *S. aureus*, cell survivability decreased on the untreated mortar surfaces, which can be attributed to cell wall lysis processes that occur at the basic pH of this material (ranging from 10 to 12). Similar observations have been made by other authors when fresh mortars are compared to carbonated ones [13], where pH drops to the 8–9 range. According to our measurements with pH strips, the water in contact with the untreated surface (60 s) showed pH of 10.5–11.0. On the other hand, the samples coated with HYDRO generally presented a lower reduction of cell survivability, and a growing trend was even observed for *E. coli* and *S. aureus*. Although hydrophobic coatings are known to decrease bioreceptivity of porous materials by limiting water availability, this factor seems to be of minor relevance under our experiment conditions, where it can be offset by the surface properties. The pH measurement of the coated surfaces indicated a value of 8.5–9.0, attributable to the acidic nature of the silica gel and a lower interaction of the cement phases with water. In addition, the higher initial cell attachment observed for some organisms may contribute to this observation.

The effect of the biocide component on the mortars treated with BIOC was only observed for *S. cerevisiae*, *S. aureus* and *P. fluorescens*, and the decreases in t[ATP] are not directly correlated to the EC50 values of the Ag/N–SiO_2NPs, indicating that surface phenomena and interactions with the cells had a greater impact than susceptibility to Ag. Interestingly, the microorganisms where the effect of the biocide was observed are those which showed the highest differences in initial cell attachment (t[ATP] values at 2 h) between HYDRO and BIOC surfaces. As reported by different authors [47,48], promoting a better contact of biocides with the cell wall via electrostatic or other interactions can increase their effectiveness. This observation is in line with our previous works [39,45], where it was observed that similar coatings (applied on stone) presented a higher inhibitory effect when the Ag/SiO_2 particles were functionalized to present a positive charge. Therefore, the higher attachment of the microorganisms, compared to HYDRO, due to the surface properties of BIOC can be offset by the biocide agent (Ag/N–SiO_2NPs) as long as its contact with the cell walls is favored. It should be noted that, the measurements after 24 h may also be affected the deposition of organic components from the culture media or secretion of extracellular substances, as suggested by the presence of deposits observed in the SEM micrographs (Fig. S3). These exogenous materials

may alter the surface properties (e.g. charge, surface energy), cell viability or interact with the biocide decreasing its effect (e.g. complexation of Ag^{+} ions by –SH of $–NH_x$ groups).

4. Conclusions

Antimicrobial effectiveness of the studied multifunctional superhydrophobic/biocide ormosil coatings, formulated for cementitious materials, depends simultaneously on a complex combination of effects related to the surface properties (electrostatic charge, surface energy, wetting, pH, topography), microorganism species and effectiveness of the biocide (toxicity of the component, interaction with cell walls). To study these factors, a comparison was made with the untreated mortar and a hydrophobic coating without the biocide component (functionalized Ag/SiO_2 nanoparticles). The effect of the silica particles functionalization with $–NH_x$ groups ($Ag/N–SiO_2$) was also assessed by comparison with bare Ag/SiO_2.

Under conditions where water availability is not a limiting factor for cell growth, it was found that hydrophobic and superhydrophobic coatings may lead to an undesired increase of cell attachment at the early biofilm formation stages, which limits the anti-fouling effectiveness of the coating.

In general terms, the surface tension calculations indicated that the cell-substrate adhesion forces via non-specific interactions are higher on hydrophobic surfaces than hydrophilic ones, especially for microorganisms with a less polar cell wall. The effect of the surface energy dispersive component is minor in comparison to the polar component. The contribution of these forces has been observed experimentally in the ATP measurements of the surfaces after 2 h in contact with the cell cultures, although it may be offset by opposing factors, mainly the decrease in surface porosity and smoother profile of the coated surface. The type of cells was found relevant on this balance, as the attachment to the hydrophobic surface was more favored for the *Gram* + bacteria and yeast. Further studies would be necessary to identify whether this effect is mediated by specific interactions. In comparison with the hydrophobic surface, the superhydrophobic one showed a higher tendency to initial cell attachment, as it switches to a Wenzel wetting state, increasing the effective contact area due its higher nano-roughness. This difference was more marked in the non-motile microorganisms.

An evident effect of the electrostatic charge (from the z-potential values) was observed for the interaction of the biocide nanoparticles with the cells, where functionalization with positively charged groups increases cell-particle contact. The magnitude of this interaction, however, is not proportional to the z-potential of the cells, which suggests the influence of cell-specific mechanisms. In general terms, the positive charge increased the biocide effect of the Ag/SiO_2 particles during the micro-dilution assay, although aggregation phenomena should be considered. Similarly, it was found that the biocide effect of the coating with $Ag/N–SiO_2$ particles (after incubation for 24 h) increased for the microorganisms where electrostatic interactions showed a higher effect, suggesting that contact with the biocide plays a key role. Toxicity of the silver itself could not explain the trends observed for the coating.

The results of this work highlight how the use of hydrophobic and superhydrophobic coatings as anti-biofouling strategies should be carefully considered depending on the substrate properties and working conditions, as there are different factors that can make them more susceptible to initial stages of colonization. The combination with biocide nanoparticles can offset such effects by inhibiting subsequent cell growth, but their effectiveness is similarly affected by cell-surface interactions, which greatly vary between different microorganisms. Thus, the insight obtained about how the cell and surface properties affect the interactions may help in the design and optimization of coatings tailored to different materials and applications.

CRediT authorship contribution statement

Rafael Zarzuela: Conceptualization, Formal analysis, Investigation, Methodology, Writing – original draftWriting – original draft. **Marcia Domínguez:** Conceptualization, Formal analysis, Investigation, Methodology. **María Carbú:** Conceptualization, Formal analysis, Methodology, Writing – review & editingWriting – review & editing. **Ignacio Moreno-Garrido:** Conceptualization, Formal analysis, Methodology, Writing – review & editingWriting – review & editing. **Ana Diaz:** Formal analysis, Investigation. **Jesús M. Cantoral:** Project administration, Supervision. **M.L. Almoraima Gil:** Visualization, Writing – review & editingWriting – review & editing, Supervision. **María J. Mosquera:** Funding acquisition, Project administration.

Declaration of competing interest

The authors declare that they have no known competing financial interests or personal relationships that could have appeared to influence the work reported in this paper.

Data availability

No data was used for the research described in the article.

Acknowledgements

This work has been financed by the Spanish State Research Agency (MCIN/AEI/ 10.13039/501100011033) R&D programs 2020–2021 (Project references: PID2020-115843RB-I00 and PDC2021-121652-I00); This work has been co-financed by the European Union under the 2014–2020 ERDF Operational Programme and by the Department of Economic Transformation, Industry, Knowledge, and Universities of the Regional Government of Andalusia (Project reference: FEDER- UCA18-106613)

Appendix A. Supplementary data

Supplementary data to this article can be found online at https://doi.org/10.1016/j.buildenv.2023.110707.

References

[1] B. Stephens, P. Azimi, M.S. Thoemmes, M. Heidarinejad, J.G. Allen, J.A. Gilbert, Microbial exchange via fomites and implications for human health, Curr. Pollut. Reports. 5 (2019) 198–213, https://doi.org/10.1007/s40726-019-00123-6.
[2] P.A. Borrusso, J.J. Quinlan, Prevalence of pathogens and indicator organisms in home kitchens and correlation with unsafe food handling practices and conditions, J. Food Protect. 80 (2017) 590–597, https://doi.org/10.4315/0362-028X.JFP-16-354.
[3] A. Ghaffarianhoseini, H. AlWaer, H. Omrany, A. Ghaffarianhoseini, C. Alalouch, D. Clements-Croome, J. Tookey, Sick building syndrome: are we doing enough? Architect. Sci. Rev. 61 (2018) 99–121, https://doi.org/10.1080/00038628.2018.1461060.
[4] T. Ahmed, M. Usman, M. Scholz, Biodeterioration of buildings and public health implications caused by indoor air pollution, Indoor Built Environ. 27 (2018) 752–765, https://doi.org/10.1177/1420326X17690912.
[5] A. Mccormick, J. Loeffler, F. Ebel, Aspergillus fumigatus: contours of an opportunistic human pathogen, Cell, Microbiol. 12 (2010) 1535–1543, https://doi.org/10.1111/j.1462-5822.2010.01517.x.
[6] T. Warscheid, J. Braams, Biodeterioration of stone: a review, Int. Biodeterior. Biodegrad. 46 (2000) 343–368, https://doi.org/10.1016/S0964-8305(00)00109-8.
[7] S. Manso, M.Á. Calvo-Torras, N. De Belie, I. Segura, A. Aguado, Evaluation of natural colonisation of cementitious materials: effect of bioreceptivity and environmental conditions, Sci. Total Environ. 512–513 (2015) 444–453, https://doi.org/10.1016/j.scitotenv.2015.01.086.
[8] S. Wei, Z. Jiang, H. Liu, D. Zhou, M. Sanchez-Silva, Microbiologically induced deterioration of concrete - a review, Braz. J. Microbiol. 44 (2013) 1001–1007, https://doi.org/10.1590/S1517-83822014005000006.
[9] T.R. Munyai, T. Sonqishe, J.R. Gumbo, Algae colonisation of brick pavement at the University of Venda: a potential slippery hazard, Jamba J. Disaster Risk Stud 11 (2019) 1–7, https://doi.org/10.4102/jamba.v11i2.689.

[10] F.P. Glasser, J. Marchand, E. Samson, Durability of concrete — degradation phenomena involving detrimental chemical reactions, Cement Concr. Res. 38 (2008) 226–246, https://doi.org/10.1016/j.cemconres.2007.09.015.

[11] L. Bertolini, B. Elsener, P. Pedeferri, R. Polder, Corrosion of Steel in Concrete: Prevention, Diagnosis, Repair, Wiley-VCH, 2013.

[12] T. Verdier, M. Coutand, A. Bertron, C. Roques, A review of indoor microbial growth across building materials and sampling and analysis methods, Build. Environ. 80 (2014) 136–149, https://doi.org/10.1016/j.buildenv.2014.05.030.

[13] T. Noeiaghaei, A. Mukherjee, N. Dhami, S.R. Chae, Biogenic deterioration of concrete and its mitigation technologies, Construct. Build. Mater. 149 (2017) 575–586, https://doi.org/10.1016/j.conbuildmat.2017.05.144.

[14] R. Campana, L. Sabatini, E. Frangipani, Moulds on cementitious building materials—problems, prevention and future perspectives, Appl. Microbiol. Biotechnol. 104 (2020) 509–514, https://doi.org/10.1007/s00253-019-10185-7.

[15] P. Nowicka-Krawczyk, M. Komar, B. Gutarowska, Towards understanding the link between the deterioration of building materials and the nature of aerophytic green algae, Sci. Total Environ. 802 (2022), https://doi.org/10.1016/j.scitotenv.2021.149856.

[16] O. Ortega-Morales, J.L. Montero-Muñoz, J.A. Baptista Neto, I.B. Beech, J. Sunner, C. Gaylarde, Deterioration and microbial colonization of cultural heritage stone buildings in polluted and unpolluted tropical and subtropical climates: a meta-analysis, Int. Biodeterior. Biodegrad. 143 (2019), 104734, https://doi.org/10.1016/j.ibiod.2019.104734.

[17] J.J. Ortega-Calvo, M. Hernandez-Marine, C. Saiz-Jimenez, Biodeterioration of building materials by cyanobacteria and algae, Int. Biodeterior. 28 (1991) 165–185, https://doi.org/10.1016/0265-3036(91)90041-O.

[18] T.C. Dakal, S.S. Cameotra, Microbially induced deterioration of architectural heritages: routes and mechanisms involved, Environ. Sci. Eur. 24 (2012) 1–13, https://doi.org/10.1186/2190-4715-24-36.

[19] A.F. Halbus, T.S. Horozov, V.N. Paunov, Colloid particle formulations for antimicrobial applications, Adv. Colloid Interface Sci. 249 (2017) 134–148, https://doi.org/10.1016/j.cis.2017.05.012.

[20] L. Chen, J. Liang, An overview of functional nanoparticles as novel emerging antiviral therapeutic agents, Mater. Sci. Eng., C 112 (2020), 110924, https://doi.org/10.1016/j.msec.2020.110924.

[21] M. Rai, S.D. Deshmukh, A.P. Ingle, I.R. Gupta, M. Galdiero, S. Galdiero, Metal nanoparticles: the protective nanoshield against virus infection, Crit. Rev. Microbiol. 42 (2016) 46–56, https://doi.org/10.3109/1040841X.2013.879849.

[22] T. Naseem, T. Durrani, The role of some important metal oxide nanoparticles for wastewater and antibacterial applications: a review, Environ. Chem. Ecotoxicol. 3 (2021) 59–75, https://doi.org/10.1016/j.enceco.2020.12.001.

[23] O. Baaloudj, I. Assadi, N. Nasrallah, A. El Jery, L. Khezami, A.A. Assadi, Simultaneous removal of antibiotics and inactivation of antibiotic-resistant bacteria by photocatalysis: a review, J. Water Process Eng. 42 (2021), 102089, https://doi.org/10.1016/j.jwpe.2021.102089.

[24] I. De Pasquale, C. Lo Porto, M. Dell'Edera, F. Petronella, A. Agostiano, M.L. Curri, R. Comparelli, Photocatalytic TiO2-based nanostructured materials for microbial inactivation, Catalysts 10 (2020) 1382, https://doi.org/10.3390/catal10121382.

[25] K. Kalwar, D. Shan, Antimicrobial effect of silver nanoparticles (AgNPs) and their mechanism – a mini review, Micro & Nano Lett. 13 (2018) 277–280, https://doi.org/10.1049/mnl.2017.0648.

[26] A. Ivask, S. George, O. Bondarenko, A. Kahru, Metal-containing nano-antimicrobials: differentiating the impact of solubilized metals and particles, in: N. Cioffi, M. Rai (Eds.), Nano-Antimicrobials Prog. Prospect., first ed., Springer-Verlag Berlin Heidelberg, 2012, pp. 253–290, https://doi.org/10.1007/978-3-642-24428-5.

[27] M. Rai, A. Yadav, A. Gade, Silver nanoparticles as a new generation of antimicrobials, Biotechnol. Adv. 27 (2009) 76–83, https://doi.org/10.1016/j.biotechadv.2008.09.002.

[28] J. Blasco, I. Corsi, I. Murray, A. Fogarty, Ecotoxicology of nanoparticles in aquatic systems, in: Toxic. Nanomater., CRC Press, Taylor & Francis Group, BocaRaton, Fl, 2019, pp. 191–214, https://doi.org/10.1201/9780429265471-8.

[29] C. Yao, S. Xu, X. Jiang, J. Chen, X. Yuan, A simple way to achieve self-cleaning surfaces with unique antifouling property, J. Chem. 2020 (2020), https://doi.org/10.1155/2020/9072432.

[30] T. Martinez, A. Bertron, G. Escadeillas, E. Ringot, Algal growth inhibition on cement mortar: efficiency of water repellent and photocatalytic treatments under UV/VIS illumination, Int. Biodeterior. Biodegrad. 89 (2014), https://doi.org/10.1016/j.ibiod.2014.01.018, 1150–125.

[31] N. Encinas, C.Y. Yang, F. Geyer, A. Kaltbeitzel, P. Baumli, J. Reinholz, V. Mailänder, H.J. Butt, D. Vollmer, Submicrometer-sized roughness suppresses bacteria adhesion, ACS Appl. Mater. Interfaces (2020), https://doi.org/10.1021/acsami.9b22621.

[32] S. Zheng, M. Bawazir, A. Dhall, H.E. Kim, L. He, J. Heo, G. Hwang, Implication of surface properties, bacterial motility, and hydrodynamic conditions on bacterial surface sensing and their initial adhesion, Front. Bioeng. Biotechnol. 9 (2021) 1–22, https://doi.org/10.3389/fbioe.2021.643722.

[33] P. Zhang, L. Lin, D. Zang, X. Guo, M. Liu, Designing bioinspired anti-biofouling surfaces based on a superwettability strategy, Small 13 (2016), 1503334, https://doi.org/10.1002/smll.201503334.

[34] S. Pechook, K. Sudakov, I. Polishchuk, I. Ostrov, V. Zakin, B. Pokroy, M. Shemesh, Bioinspired passive anti-biofouling surfaces preventing biofilm formation, J. Mater. Chem. B 3 (2015) 1371–1378, https://doi.org/10.1039/C4TB01522C.

[35] W. Liu, L. Zhuang, J. Liu, Y. Liu, L. Wang, Y. He, G. Yang, F. Shen, X. Zhang, Y. Zhang, Make the building walls always clean : a durable and anti-bioadhesive diatomaceous earth @ SiO 2 coating, Construct. Build. Mater. 301 (2021), 124293, https://doi.org/10.1016/j.conbuildmat.2021.124293.

[36] H.K. Webb, S.N. Ha, R.J. Crawford, E.P. Ivanova, Biological interactions with superhydrophobic surfaces, in: R.J. Crawford, E.P. Ivanova (Eds.), Superhydrophobic Surfaces, Elsevier Inc., Amsterdam, 2015, pp. 151–160, https://doi.org/10.1016/B978-0-12-801109-6.00003-3.

[37] J.K. Oh, Y. Yegin, F. Yang, M. Zhang, J. Li, S. Huang, S.V. Verkhoturov, E. A. Schweikert, K. Perez-Lewis, E.A. Scholar, T.M. Taylor, A. Castillo, L. Cisneros-Zevallos, Y. Min, M. Akbulut, The influence of surface chemistry on the kinetics and thermodynamics of bacterial adhesion, Sci. Rep. 8 (2018) 1–13, https://doi.org/10.1038/s41598-018-35343-1.

[38] R.J. Crawford, H.K. Webb, V.K. Truong, J. Hasan, E.P. Ivanova, Surface topographical factors influencing bacterial attachment, Adv. Colloid Interface Sci. 179–182 (2012) 142–149, https://doi.org/10.1016/j.cis.2012.06.015.

[39] M. Domínguez, R. Zarzuela, I. Moreno-Garrido, M. Carbú, J.M.J.M. Cantoral, M.J. M.J. Mosquera, M.L.A.A. Gil, Anti-fouling nano-Ag/SiO2 ormosil treatments for building materials: the role of cell-surface interactions on toxicity and bioreceptivity, Prog. Org. Coating 153 (2021), 106120, https://doi.org/10.1016/j.porgcoat.2020.106120.

[40] M. Spasova, N. Manolova, N. Markova, I. Rashkov, Superhydrophobic PVDF and PVDF-HFP nanofibrous mats with antibacterial and anti-biofouling properties, Appl. Surf. Sci. 363 (2016) 363–371, https://doi.org/10.1016/j.apsusc.2015.12.049.

[41] S. Liu, J. Zheng, L. Hao, Y. Yegin, M. Bae, B. Ulugun, T.M. Taylor, E.A. Scholar, L. Cisneros-Zevallos, J.K. Oh, M. Akbulut, Dual-functional, superhydrophobic coatings with bacterial anticontact and antimicrobial characteristics, ACS Appl. Mater. Interfaces (2020), https://doi.org/10.1021/acsami.9b18928.

[42] S. Heinonen, E. Huttunen-Saarivirta, J.P. Nikkanen, M. Raulio, O. Priha, J. Laakso, E. Storgårds, E. Levänen, Antibacterial properties and chemical stability of superhydrophobic silver-containing surface produced by sol-gel route, Colloids Surfaces A Physicochem. Eng. Asp. 453 (2014) 149–161, https://doi.org/10.1016/j.colsurfa.2014.04.037.

[43] T. Liu, B. Yin, T. He, N. Guo, L. Dong, Y. Yin, Complementary effects of nanosilver and superhydrophobic coatings on the prevention of marine bacterial adhesion, ACS Appl. Mater. Interfaces 4 (2012) 4683–4690, https://doi.org/10.1021/am301049v.

[44] B. Yin, T. Liu, Y. Yin, Prolonging the duration of preventing bacterial adhesion of nanosilver-containing polymer films through hydrophobicity, Langmuir 28 (2012) 17019–17025, https://doi.org/10.1021/la303264k.

[45] R. Zarzuela, M. Carbú, M.L.A. Gil, J.M. Cantoral, M.J. Mosquera, Ormosils loaded with SiO2 nanoparticles functionalized with Ag as multifunctional superhydrophobic/biocidal/consolidant treatments for buildings conservation, Nanotechnology 30 (2019), 345701, https://doi.org/10.1088/1361-6528/ab1ff0.

[46] R. Zarzuela, M. Carbú, A. Gil, J. Cantoral, M.J. Mosquera, Incorporation of functionalized Ag-TiO2NPs to ormosil-based coatings as multifunctional biocide, superhydrophobic and photocatalytic surface treatments for porous ceramic materials, Surface. Interfac. 25 (2021), 101257, https://doi.org/10.1016/j.surfin.2021.101257.

[47] A. Verma, F. Stellacci, Effect of surface properties on nanoparticle-cell interactions, Small 6 (2010) 12–21, https://doi.org/10.1002/smll.200901158.

[48] Y.N. Slavin, J. Asnis, U.O. Häfeli, H. Bach, Metal nanoparticles: understanding the mechanisms behind antibacterial activity, J. Nanobiotechnol. 15 (2017) 1–20, https://doi.org/10.1186/s12951-017-0308-z.

[49] D.H. Kaelble, Dispersion-polar surface tension properties of organic solids, J. Adhes. 2 (1970) 66–81, https://doi.org/10.1080/0021846708544582.

[50] A. Alghunaim, S. Kirdponpattara, B.M.Z. Newby, Techniques for determining contact angle and wettability of powders, Powder Technol. 287 (2016) 201–215, https://doi.org/10.1016/j.powtec.2015.10.002.

[51] H.J. Busscher, A.H. Weerkamp, H.C. van der Mei, A.W. van Pelt, H.P. de Jong, J. Arends, Measurement of the surface free energy of bacterial cell surfaces and its relevance for adhesion, Appl. Environ. Microbiol. 48 (1984) 980–983, https://doi.org/10.1128/AEM.48.5.980-983.1984.

[52] "Quest Graph™ EC50 Calculator." AAT Bioquest, Inc., (n.d.). https://www.aatbio.com/tools/ec50-calculator (accessed March 16, 2022).

[53] S. Suppi, K. Kasemets, A. Ivask, K. Künnis-Beres, M. Sihtmäe, I. Kurvet, V. Aruoja, A. Kahru, A novel method for comparison of biocidal properties of nanomaterials to bacteria, yeasts and algae, J. Hazard Mater. 286C (2014) 75–84, https://doi.org/10.1016/j.jhazmat.2014.12.027.

[54] I. Garcia-Lodeiro, P.M.M. Carmona-Quiroga, R. Zarzuela, M.J. Mosquera, M.T. T. Blanco-Varela, Chemistry of the interaction between an alkoxysilane-based impregnation treatment and cementitious phases, Cement Concr. Res. 142 (2021), 106351, https://doi.org/10.1016/j.cemconres.2020.106351.

[55] R.N. Wenzel, Resistance of solid surfaces to wetting by water, J. Ind. Eng. Chem. (Washington, D. C.). 28 (1936) 988–994, https://doi.org/10.1021/ie50320a024.

[56] D. Kim, N.M. Pugno, S. Ryu, Wetting theory for small droplets on textured solid surfaces, Sci. Rep. 6 (2016) 1–8, https://doi.org/10.1038/srep37813.

[57] F. Cirisano, A. Benedetti, L. Liggieri, F. Ravera, E. Santini, M. Ferrari, Amphiphobic coatings for antifouling in marine environment, Colloids Surfaces A Physicochem. Eng. Asp. 505 (2016) 158–164, https://doi.org/10.1016/j.colsurfa.2016.03.045.

[58] Xiaoxue Zhang, L. Wang, E. Levänen, Superhydrophobic surfaces for reduction of bacterial adhesion, RCS Adv 3 (2013) 12003–12020, https://doi.org/10.1039/c3ra40497h.

[59] A.J. Scardino, E. Harvey, R. De Nys, Testing attachment point theory: diatom attachment on microtextured polyimide biomimics, Biofouling 22 (2006) 55–60, https://doi.org/10.1080/08927010500506094.

[60] E.W. Washburn, The dynamics of capillary flow, Phys. Rev. 17 (1921) 273–283, https://doi.org/10.1103/PhysRev.17.273.
[61] T.J. Silhavy, D. Kahne, S. Walker, The bacterial cell envelope, Cold Spring Harbor Perspect. Biol. 2 (2010) 1–16, https://doi.org/10.1101/cshperspect.a000414.
[62] P.N. Lipke, R. Ovalle, Cell wall architecture in yeast : new structure and new challenges, J. Bacteriol. 180 (1998) 3735–3740.
[63] S. Halder, K.K. Yadav, R. Sarkar, S. Mukherjee, P. Saha, S. Haldar, S. Karmakar, T. Sen, Alteration of Zeta potential and membrane permeability in bacteria: a study with cationic agents, SpringerPlus 4 (2015) 1–14, https://doi.org/10.1186/s40064-015-1476-7.
[64] J. Wingender, T.R. Neu, H.-C. Flemming (Eds.), Microbial Extracellular Polymeric Substances, Springer Berlin Heidelberg, Berlin, Heidelberg, 1999, https://doi.org/10.1007/978-3-642-60147-7.
[65] A. Celani, M. Vergassola, Bacterial strategies for chemotaxis response, Proc. Natl. Acad. Sci. USA 107 (2010) 1391–1396, https://doi.org/10.1073/pnas.0909673107.
[66] R. Zarzuela, I. Moreno-Garrido, M.L.A.A. Gil, M.J.M.J. Mosquera, Effects of surface functionalization with alkylalkoxysilanes on the structure, visible light photoactivity and biocidal performance of Ag-TiO2 nanoparticles, Powder Technol. 383 (2021) 381–395, https://doi.org/10.1016/j.powtec.2021.01.050.
[67] A.Z. Miller, P. Sanmartín, L. Pereira-Pardo, A. Dionísio, C. Saiz-Jimenez, M. F. Macedo, B. Prieto, Bioreceptivity of building stones: a review, Sci. Total Environ. 426 (2012) 1–12, https://doi.org/10.1016/j.scitotenv.2012.03.026.
[68] Y. Elakneswaran, T. Nawa, K. Kurumisawa, Electrokinetic potential of hydrated cement in relation to adsorption of chlorides, Cement Concr. Res. 39 (2009) 340–344, https://doi.org/10.1016/j.cemconres.2009.01.006.
[69] E. Yogarajah, T. Nawa, K. Kurumisawa, K. Fushimi, Surface charge of hardened cement paste determined by membrane potential, Cem. Sci. Concr. Technol. Japan Cem. Assoc. 60 (2018) 111–117.